Biochemical Journal (2019) **476** 483–497
https://doi.org/10.1042/BCJ20180801

Research Article

CGA-N9, an antimicrobial peptide derived from chromogranin A: direct cell penetration of and endocytosis by *Candida tropicalis*

Ruifang Li[1], Chen Chen[1], Sha Zhu[2], Xueqin Wang[1], Yanhui Yang[1], Weini Shi[1], Sijia Chen[1], Congcong Wang[1], Lixing Yan[1] and Jiaofan Shi[1]

[1]College of Biological Engineering, Henan University of Technology, Zhengzhou 450001, China; [2]Department of Immunology, Key Laboratory of Infection and Immunization, College of Basic Medical Sciences, Zhengzhou University, Zhengzhou, Henan 450001, China

Correspondence: Ruifang Li (lrf@haut.edu.cn)

CGA-N9 is a peptide derived from the N-terminus of human chromogranin A comprising amino acids 47–55. Minimum inhibitory concentration (MIC) assays showed that CGA-N9 had antimicrobial activity and exhibited time-dependent inhibition activity against *Candida tropicalis*, with high safety in human red blood cells (HRBCs) and mouse brain microvascular endothelial cells (bEnd.3). According to the results of transmission electron microscopy (TEM), flow cytometry and confocal microscopy, CGA-N9 accumulated in cells without destroying the integrity of the cell membrane; the peptide was initially localized to the cell membrane and subsequently internalized into the cytosol. An investigation of the cellular internalization mechanism revealed that most CGA-N9 molecules entered the yeast cells, even at 4°C and in the presence of sodium azide (NaN_3), both of which block all energy-dependent transport mechanisms. In addition, peptide internalization was affected by the endocytic inhibitors 5-(*N*-ethyl-*N*-isopropyl)-amiloride (EIPA), cytochalasin D (CyD) and heparin; chlorpromazine (CPZ) also had some effect on CGA-N9 internalization. Similar results were obtained in the MIC assays, whereby the anticandidal activity of CGA-N9 was blocked to different degrees in the presence of EIPA, CyD, heparin or CPZ. Therefore, most CGA-N9 passes through the *C. tropicalis* cell membrane via direct cell penetration, whereas the remainder enters through macropinocytosis and sulfate proteoglycan-mediated endocytosis, with a slight contribution from clathrin-mediated endocytosis.

Introduction

Candida is regarded as the third most common pathogen responsible for clinical diseases ranging from superficial infections of the vaginal and oral mucosa to life-threatening systemic diseases in immunocompromised patients [1–3]. *Candida tropicalis* has become one of the most common clinical species of this genus, after *Candida albicans*, causing ∼3–66% of clinical candidiasis, especially in America and Asia [4–6]. With the continuous emergence of conventional antibiotic-resistant strains, the morbidity and mortality rates due to candidiasis are gradually increasing [1,7]. Thus, there is an urgent need to discover novel and more effective antifungal agents to combat potentially fatal pathogenic fungi [8–10].

Based on their advantages over the limited number of clinical compounds used to treat fungal infections and the side effects of conventional antifungal drugs, antimicrobial peptides (AMPs) have received much attention in recent years and show a wide range of activity, low toxicity and low resistance development [11]. Various AMPs with diverse structures and antimicrobial properties have been discovered from different sources, such as plants, animals and microorganisms [12–15].

Received: 8 October 2018
Revised: 22 December 2018
Accepted: 4 January 2019

Accepted Manuscript online: 4 January 2019
Version of Record published: 5 February 2019

Biochemical Journal (2019) **476** 483–497
https://doi.org/10.1042/BCJ20180801

Chromogranin A (CGA), a member of the chromogranin family, is ubiquitously distributed in the chromaffin granules of neuroendocrine cells. It is highly conserved and widely presents in many mammals, such as humans, bovine and mice, especially in the N-terminal and C-terminal regions [16]. CGA exhibits antibacterial and antifungal activities, particularly in the N-terminal domain [17]. CGA-derived peptides are involved in innate immunity [18]. In this study, we identified the AMP CGA-N9, which is an N-terminal derivative of human CGA consisting of amino acids 47–55.

The first target of AMPs is the cell membrane [19–21]. The electrostatic interaction between the peptide and cell membrane, followed by entry via the membrane and effects on intracellular organelles, appears to be the basic mechanism by which most AMPs perform their antimicrobial function [19,22,23]. Although the mechanism of action of most AMPs is reported to include membrane lysis and intracellular activity [24–29], the exact membrane process responsible for non-pore-dependent mechanisms remains poorly understood due to the complicated physical and chemical properties of these peptides.

Here, we investigate the routes by which CGA-N9 enters *C. tropicalis*.

Materials and methods

Microorganisms, cell line and reagents

Candida glabrata (ATCC90525), *Candida parapsilosis* (ATCC20224), *Candida krusei* (ATCC6258), *C. tropicalis* (ATCC20138), *Candida albicans* (ATCC2048), *Cryptococcus neoformans* (ATCC14116), *Escherichia coli* (ATCC25922), *Staphylococcus aureus* (ATCC25923), *Bacillus subtilis* (ATCC5230), *Listeria monocytogenes* (ATCC13932) and *Pseudomonas aeruginosa* (ATCC35554) were supplied by the China Academy of Chinese Medical Sciences (Beijing, China). Fungi were sub-cultured onto Sabouraud dextrose (SD) agar at 30°C for 48 h. Bacteria were cultured on Luria-Bertani (LB) agar at 37°C for 16 h. The bacteria and fungi were maintained at 4°C for short-term storage.

The mouse brain microvascular endothelial cell line (bEnd.3) was provided by the Shaanxi Key Laboratory of Natural Products Chemistry and Biology, College of Chemistry & Pharmacy, Northwest A&F University.

CGA-N9 (NH_2-RILSILRHQ-COOH) was synthesized using a solid-phase method. One milligram of peptide was dissolved in 15 μl of dimethyl sulfoxide, and 985 μl of phosphate-buffered saline (PBS) (20 mmol/l, pH 6.0) was added to a total volume of 1 ml; an appropriately diluted sample was used for subsequent analysis.

Antimicrobial assay

The antimicrobial activity of peptide CGA-N9 was evaluated by employing the broth micro-dilution method [30], with minor modifications. In brief, fungi were cultured in SD liquid medium at 28°C for logarithmic growth, and bacteria were cultured in LB liquid medium at 37°C for logarithmic growth. Cells were suspended in medium, and the concentration was adjusted to 1×10^6 cfu/ml for fungal inocula and 1×10^5 cfu/ml for bacterial inocula. A 100-μl volume of CGA-N9 solution (1 mg/ml) was added to the wells of a 96-well plate and serially diluted twofold with PBS. The final concentrations of the peptide mixture ranged from 1000 to 1.95 μg/ml. Each well was inoculated with equal volumes of microbial cells. After incubation for 16 h for bacteria and 20 h for fungi, 10 μl of 3-(4,5-dimethylthiazol-2-yl)-2,5-diphenyltetrazolium (MTT) solution (5 mg/ml in PBS) was added to each well to detect live cells. Absorbance at 570 nm (A_{570}) was measured. The MIC_{100} was defined as the lowest concentration resulting in no visible growth compared with control cells [7]. The cytotoxicity kinetics of CGA-N9 against *C. tropicalis* was defined as the cell viability kinetics measured at 4-h intervals. Experiments were conducted in triplicate.

Fungicidal assay

The minimum fungicidal concentration (MFC) was determined following the incubation of CGA-N9 with *C. tropicalis* in the MIC assay by removing 150 μl of sample from each well, plating the samples onto SD agar plates and culturing for 20–36 h at 28°C. The resulting colonies were counted. MFC was defined as the lowest concentration of CGA-N9 that killed 99.9% of the initial inoculum [25].

Hemolytic assay

The hemolytic activity of CGA-N9 was tested by a previously reported method [31]. Briefly, fresh HRBCs (human red blood cells) from healthy volunteers were washed thrice with normal saline, and HRBS suspensions were prepared at a final concentration of 2% for this assay. One hundred microliters of double-diluted

CGA-N9 (0–500 μg/ml) was added to each well of a 96-well plate, followed by 100 μl of 2% HRBC suspension in each well. After incubation for 30 min at 37°C, 150 μl of supernatant was transferred to a new 96-well plate, and the amount of hemoglobin released at 540 nm was measured. One-percent Triton X-100 was used as a positive control, and normal saline was used as a negative control. The percentage of hemolysis was calculated by the following equation:

$$\text{hemolysis (\%)} = (\text{sample } A_{540} - \text{negative control } A_{540})/(\text{positive control } A_{540} - \text{negative control } A_{540})$$

Cell counting kit-8 method

An *in vitro* mammalian cell cytotoxicity test of CGA-N9 was performed with a mouse brain microvascular endothelial cell line (bEnd.3) using the CCK8 method (Cell Counting Kit-8) [32,33]. 4×10^3 bEnd.3 cells were seeded in each well of a 96-well plate. After the cells were incubated at 37°C in 5% CO_2 for 10 h, different concentrations of CGA-N9 (0–80 times the MIC_{100}) were added in the wells and further incubated for 48 h. The toxicity of CGA-N9 towards bEnd.3 cells was determined using CCK8 (MedChem Express, Shanghai, China). Absorbance was measured by an ELISA plate reader at 450 nm. Cells that were not incubated with CGA-N9 were used as a negative control, and DMEM containing 5% FBS was used as a blank control. Cell viability was calculated with the following equation:

$$\text{cell viability (\%)} = (\text{sample } A_{450} - \text{blank control } A_{450})/(\text{negative control } A_{450} - \text{blank control } A_{450})$$

Transmission electron microscopy

C. tropicalis cells were observed by transmission electron microscopy (TEM) after CGA-N9 treatment [28]. Briefly, 1×10^6 cfu/ml mid-log phase *C. tropicalis* cells were incubated with CGA-N9 at a concentration of 3.9 μg/ml (MIC_{100}) at 28°C. *C. tropicalis* cells in 1 ml of culture were collected after each 4-h interval and fixed overnight in 500 μl of 5% glutaraldehyde in PBS at 4°C. The cells were then further fixed in 1 ml of osmium acid for 1.5 h at room temperature. The samples were dehydrated and embedded in resin. Ultra-thin sections were stained with uranyl acetate followed by lead citrate. The specimens were observed by TEM (Hitachi H-7650; Hitachi, Ltd, Tokyo, Japan). *C. tropicalis* cells that had not been exposed to CGA-N9 were used as controls.

Flow cytometry

Propidium iodide (PI) can bind nucleic acids after penetrating the compromised cell membrane of dead, membrane-damaged and apoptotic cells. The effect of CGA-N9 on the membrane permeability of *C. tropicalis* was determined by flow cytometry using PI and the method outlined by Li et al. [28]. Briefly, 1×10^6 cfu/ml logarithmic *C. tropicalis* cells in SD broth were incubated with CGA-N9 (3.9 μg/ml) at 28°C. After incubation for 4, 8, 12 and 16 h, the cells were incubated with 50 μg/ml PI in the dark for more than 10 min at room temperature. The samples were analyzed using a FACSCalibur flow cytometer (BD, NJ, U.S.A.). *C. tropicalis* cells that had not undergone treatment with CGA-N9 or had been treated with 0.3% Triton X-100 were used as negative or positive controls, respectively. The results were analyzed using the FACSDiva version 6.1.3 software package.

Calcein leakage assay

The effect of CGA-N9 on the membrane integrity of *C. tropicalis* was characterized according to the leakage rate of calcein from liposomes. Calcein-loaded liposomes were prepared according to a previously reported method [34] with minor modifications. Dioleoyl phosphatidylcholine and dioleoyl phosphoethanolamine (Sigma–Aldrich, Shanghai, China) (1 : 1.27, w/w) were employed to mimic the logarithmic-phase *Candida* lipid bilayer [35]. A suspension of calcein-loaded liposomes was incubated with 3.9 μg/ml CGA-N9 at 28°C to evaluate pore formation and membrane integrity by measuring dye leakage every 1 h using a fluorescence spectrophotometer (Cary Eclipse, CA, U.S.A.) at $\lambda_{ex}/\lambda_{em}$ = 492/517 nm. In this assay, 20 mmol/l PBS (pH 7.0) was selected as a negative control, and 10 mmol/l H_2O_2 was used as a positive control. All samples were examined in triplicate. After 10 h in the presence of 0.1% Triton X-100 in Tris buffer, 100% of the dye was released from liposomes.

Biochemical Journal (2019) **476** 483–497
https://doi.org/10.1042/BCJ20180801

Peptide labeling and cellular internalization

To assess cellular uptake of CGA-N9, the peptide was labeled by covalent modification of its N-terminus with fluorescein 5-isothiocynate (FITC) using the method described by Ruissen et al. [36].

Logarithmic-phase *C. tropicalis* cells (1×10^6 cfu/ml) were incubated with the FITC-CGA-N9 conjugate at a final concentration of 2.9 μg CGA-N9/ml (MIC_{50}) at 28°C for 0, 4, 8, 12 and 16 h. After incubation, the cells were washed with pH 8.5 PBS and further incubated with 20 mmol/l Dil for 25 min to stain the cell membrane. The cells were washed and examined using a confocal laser microscope (Olympus, Tokyo, Japan) at $\lambda_{ex}/\lambda_{em}$ = 549 nm/565 nm for Dil and $\lambda_{ex}/\lambda_{em}$ = 495 nm/519 nm for FITC to observe CGA-N9 internalization.

Confocal microscopy to assay the effects of energy on cellular peptide uptake

The effects of energy on cellular peptide uptake were determined using a previously reported method [37]. A total of 1×10^6 cfu/ml logarithmic-phase *C. tropicalis* cells were pre-incubated at 4 and 30°C for 12 h with the FITC-CGA-N9 conjugate at a concentration of 2.9 μg CGA-N9/ml (MIC_{50}). The cells were examined via confocal microscopy at $\lambda_{ex}/\lambda_{em}$ = 495/519 nm. *C. tropicalis* cells that had not undergone treatment with FITC-CGA-N9 or with 0.65 mg/ml NaN_3 in the presence of FITC-CGA-N9 at 30°C for 12 h were used as negative and positive controls, respectively.

Confocal microscopy assay to identify the cellular peptide uptake pathway

Pathways involved in CGA-N9 uptake by *C. tropicalis* cells were investigated using various endocytic inhibitors [38]. First, 1×10^6 cfu/ml logarithmic-phase *C. tropicalis* cells were incubated for 1 h with one of the following endocytic inhibitors: methyl-β-cyclodextrin (Mβ-CD, 3.75 mg/ml), cytochalasin D (CyD, 5.08 μg/ml), chlorpromazine (CPZ, 7.11 μg/ml), chloroquine (CQ, 1.72 μg/ml), NaN_3 (0.65 mg/ml), 5-(*N*-ethyl-*N*-isopropyl)-amiloride (EIPA) (10 μg/ml) and heparin (100 μg/ml). The FITC-CGA-N9 conjugate at a concentration of 3.9 μg CGA-N9/ml was then added after the edocytic inhibitors were washed off, and the samples were further incubated for 12 h. Uptake of the FITC-CGA-N9 conjugate was determined using a confocal laser microscope (Olympus, Tokyo, Japan). The fluorescence value was recorded after analysis using the FV31S-SW software. Uptake of FITC-CGA-N9 by *C. tropicalis* cells in the absence of endocytic inhibitors was used as a control.

Assessment of the effects of endocytic inhibitors on peptide anticandidal activity

The effect of endocytic inhibitors on the anticandidal activity of CGA-N9 was detected by the MIC assay [38], with minor modifications. A total of 1×10^6 cfu/ml logarithmic-phase *C. tropicalis* cells were treated with Mβ-CD (3.75 mg/ml), CyD (5.08 μg/ml), CPZ (7.11 μg/ml), CQ (1.72 μg/ml), NaN_3 (0.65 mg/ml), EIPA (10 μg/ml) or heparin (100 μg/ml) for 1 h at 28°C [39]. Subsequently, CGA-N9 was added at concentrations of 1.95 μg/ml (MIC_5), 2.9 μg/ml (MIC_{50}) and 3.9 μg/ml (MIC_{100}) for 16 h at 28°C after the edocytic inhibitors were washed off, and the samples were then subjected to the MIC assay. All experiments were performed in triplicate. In this assay, 1.95 μg/ml CGA-N9 was used to identify the endocytosis inhibitors that exerted a primary effect against CGA-N9 endocytosis. The antifungal activity of CGA-N9 against *C. tropicalis* cells in the absence of endocytic inhibitors was used as a control.

Statistical analysis

SPSS version 21.0 was used for the statistical analysis (ANOVA and Tukey's test). All data are presented as the mean ± standard deviation. A P-value <0.05 indicated a difference, a P-value <0.01 indicated a significant difference and a P-value <0.001 indicated an extremely significant difference.

Results

Antimicrobial activity of CGA-N9

The cytotoxicity of CGA-N9 against microbes was determined via the MIC assay and SD agar plate culture. The MIC assay results indicated that CGA-N9 rapidly reduced the viability of *C. tropicalis* cells in a dose-dependent manner, with MIC_{50} and MIC_{100} values of 2.9 and 3.9 μg/ml, respectively (Table 1).

As shown in Figure 1, cell viability dramatically increased at CGA-N9 concentrations <3.9 μg/ml. To evaluate *C. tropicalis* viability, cells were cultured on SD agar plates after treatment with different concentrations of

Biochemical Journal (2019) **476** 483–497
https://doi.org/10.1042/BCJ20180801

Table 1 Antimicrobial spectrum of the AMP CGA-N9

MIC values were determined by MIC assay. MIC_{100} was defined as the lowest concentration resulting in no visible growth compared with control cells.

Strains	MIC_{100} (μg/ml)
C. glabrata	500.00
C. parapsilosis	250.00
C. krusei	15.63
C. tropicalis	3.90
C. neoformans	3.90
E. coli	—
S. aureus	—
B. subtilis	15.63
L. monocytogenes	31.25
P. aeruginosa	—

'—' indicates no detectable antimicrobial effect at CGA-N9 concentrations >1000 μg/ml.

CGA-N9. No colonies grew in the presence of concentrations >3.9 μg/ml, suggesting that exposure to CGA-N9 killed the *Candida* cells.

Figure 2 presents the cytotoxicity kinetics of CGA-N9. The results revealed that CGA-N9 cytotoxicity was time-dependent, with *C. tropicalis* cell killing beginning after 8 h of CGA-N9 treatment.

Hemolytic activity

The hemolytic activity of CGA-N9 (0–500 μg/ml) is revealed in Figure 3. A 5% hemolysis rate for CGA-N9 occurred at the concentration of 105.62 μg/ml (27 times the MIC_{100}). At a concentration >16 times the MIC_{100} (62.5 μg/ml), the hemolysis rate was only 0.26%. The results showed that CGA-N9 exhibits biosafety in HRBCs.

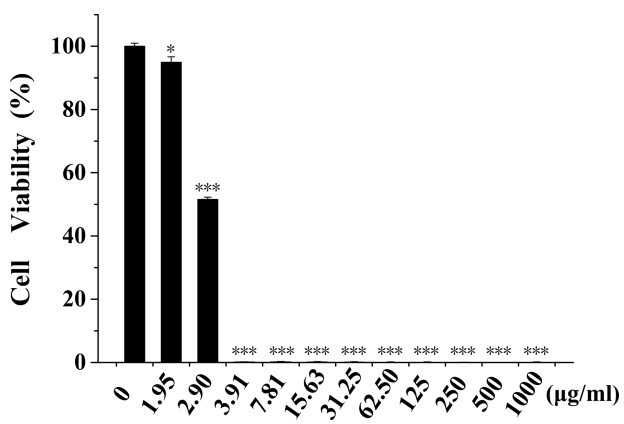

Figure 1. Cytotoxicity of CGA-N9 against *C. tropicalis* at different concentrations.

Approximately 1×10^6 logarithmic-phase *C. tropicalis* cells were incubated with CGA-N9 for 18 h at 28°C. MFC values were determined by the formation of colonies after culturing on SDA plates. MFC was defined as the lowest concentration of antifungal agent that caused at least 99.9% killing of the initial inoculum. Data represent the mean ± standard deviation of three independent experiments. $^*P < 0.05$, $^{**}P < 0.01$, $^{***}P < 0.001$ (Student's *t*-test).

Biochemical Journal (2019) **476** 483–497
https://doi.org/10.1042/BCJ20180801

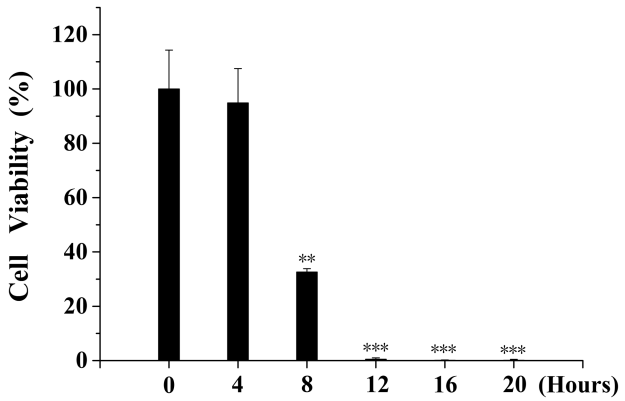

Figure 2. Cytotoxicity kinetics of CGA-N9 against *C. tropicalis*.

Approximately 1×10^6 logarithmic-phase *C. tropicalis* cells were incubated with 3.9 μg/ml CGA-N9 at 28°C. The cytotoxicity kinetics of CGA-N9 was based on the cell survival rate at different times after CGA-N9 treatment. Data represent the mean ± standard deviation of three independent experiments. $^{**}P < 0.01$, $^{***}P < 0.001$ (Student's *t*-test).

Cytotoxicity to mammalian cells

Using the CCK8 method, CGA-N9 showed non-toxicity to bEnd.3 cells after treatment for 48 h at concentrations of 10–50 times the MIC_{100}. CGA-N9 did not display any bEnd.3 cell growth inhibition until reaching concentrations of 60–80 times the MIC_{100}, at which the cell viability rate was still more than 70%. Interestingly, the viabilities of bEnd.3 cells at concentrations that were 10–40 times the MIC_{100} of CGA-N9 were higher than that of the control group, which may be due to the nutritional benefits of CGA-N9 as a peptide bEnd.3 cell growth (Figure 4). These data are sufficient to illustrate a high safety of CGA-N9 towards mammalian cells.

Ultrastructure of *C. tropicalis* cells post-treatment with CGA-N9

The impact of 3.9 μg/ml CGA-N9 on the ultrastructure of *C. tropicalis* cells was observed via TEM (Figure 5). Compared with the control, CGA-N9 exhibited time-dependent effects on *C. tropicalis* cells, which was in

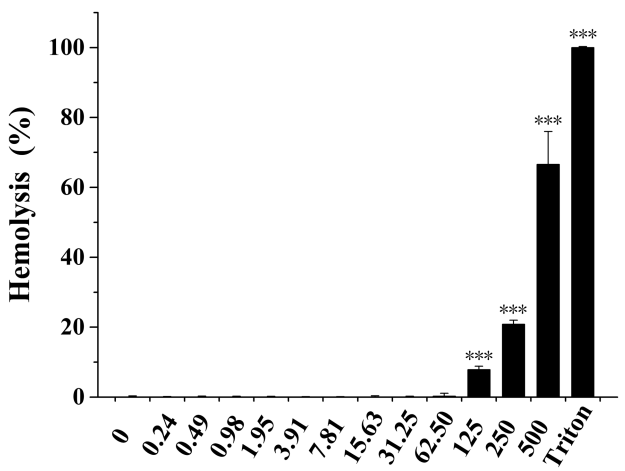

Figure 3. The hemolytic activity of CGA-N9.

The hemolysis of CGA-N9 was measured by the release of hemoglobin. HRBCs were incubated with different concentrations of CGA-N9 (0–500 μg/ml) for 30 min at 37°C. One-percent Triton X-100 was used as a positive control, and normal saline was used as a negative control. Five-percent hemolysis occurs in red blood cells post-treatment with 105.62 μg/ml CGA-N9 (27 times the MIC_{100}). Data represent the mean ± standard deviation of three independent experiments. $^{***}P < 0.001$ (Student's *t*-test).

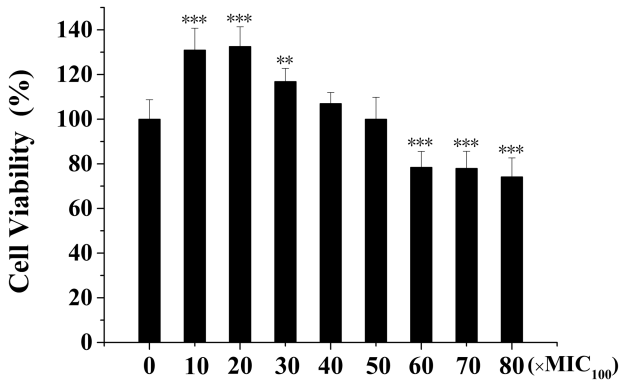

Figure 4. Cytotoxicity of CGA-N9.

Cytotoxicity of CGA-N9 to mammalian cells *in vitro* was tested by using the CCK8 method with mouse brain microvascular endothelial cells (bEnd.3). After 4×10^3 bEnd.3, cells were incubated in each well of a 96-well plate at 37°C in 5% CO_2 for 10 h, different concentrations of CGA-N9 (0–80 times the MIC_{100}) were added and further incubated for 48 h. Absorbance was measured by an ELISA plate reader at 450 nm. Cells that were not incubated with CGA-N9 were used as a negative control, and DMEM containing 5% FBS was used as a blank control. The cell viability of bEnd.3 was calculated. Data represent the mean ± standard deviation of three independent experiments. $^{**}P < 0.01$, $^{***}P < 0.001$ (Student's *t*-test).

accordance with the observed cytotoxicity kinetics. The cells displayed cytoplasmic vacuolization, mitochondrial structural damage and loss of nuclear envelope integrity after CGA-N9 treatment. Moreover, the cell wall and outer membrane of cells treated with CGA-N9 remained intact, without visible disruption, even after 16 h of treatment. These results indicate that CGA-N9 may penetrate the cell membrane without disrupting the integrity of the membrane bilayer and subsequently interact with cellular organelles.

Effects of CGA-N9 on the outer membrane permeability of *C. tropicalis* cells

PI penetrates only damaged membranes and embeds in double-stranded nucleic acids, emitting red fluorescence ($\lambda_{ex}/\lambda_{em}$ = 535 nm/615 nm); therefore, PI is widely used to detect disruption of the *C. tropicalis* outer membrane. According to our results (Figure 6), the PI fluorescent probe was unable to cross the outer membrane of *C. tropicalis* cells, even following treatment with CGA-N9 at 3.9 μg/ml for 16 h. In contrast, PI fluorescence was detected in *C. tropicalis* after treatment with the membrane-disrupting agent Triton X-100. The results suggest that CGA-N9 did not disrupt the permeability of the outer membrane of *C. tropicalis*.

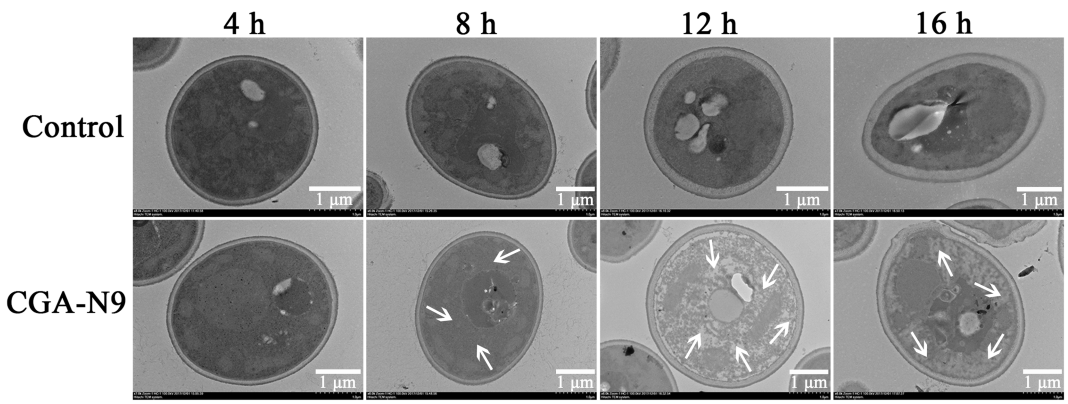

Figure 5. Effect of CGA-N9 on the ultrastructure of *C. tropicalis* cells.

A total of 1×10^6 logarithmic-phase *C. tropicalis* cells were incubated with 3.9 μg/ml CGA-N9 at 28°C for 4, 8, 12 and 16 h. Cell ultrastructure was observed via transmission electron microscopy. *C. tropicalis* cells that had not undergone CGA-N9 treatment were used as controls. Scale bar = 1 μm.

Biochemical Journal (2019) **476** 483–497
https://doi.org/10.1042/BCJ20180801

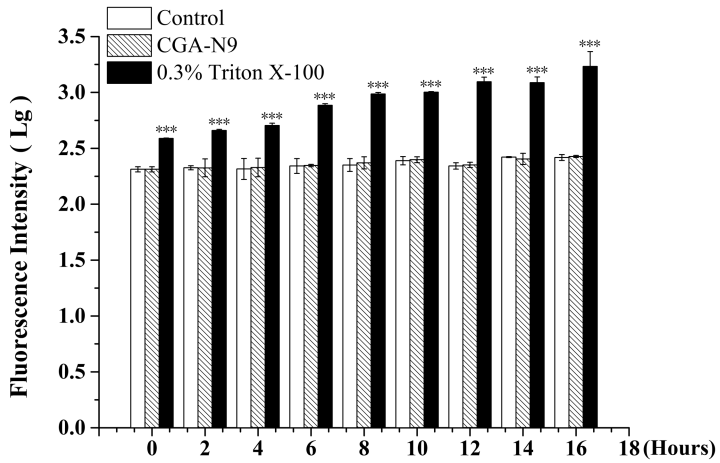

Figure 6. Effect of CGA-N9 on the outer membrane permeability of *C. tropicalis* cells.

The nucleic acid dye PI was incubated with *C. tropicalis* cells after treatment with 3.9 μg/ml CGA-N9 or 0.3% Triton X-100 at 28°C. The fluorescence of PI that had entered the cell and bound to nucleic acids was recorded using flow cytometry. An increase in fluorescence was defined as an increase in membrane permeability. Full entry was observed upon the addition of the membrane-disrupting agent Triton X-100. *C. tropicalis* cells that had not been exposed to CGA-N9 were used as controls. Data represent the mean ± standard deviation of three independent experiments. ***$P < 0.001$ (Student's *t*-test).

Effect of CGA-N9 on membrane integrity

Pore formation in the membrane was investigated by examining calcein release from liposomes treated with CGA-N9. The results showed that exposure to 3.9 μg/ml CGA-N9 did not cause leakage of calcein encased in liposomes (Figure 7), indicating that no pores were formed in the neutral liposome bilayers after treatment with CGA-N9. In contrast, complete leakage from liposomes was observed at 10 h after the addition of the membrane-disrupting agent Triton X-100.

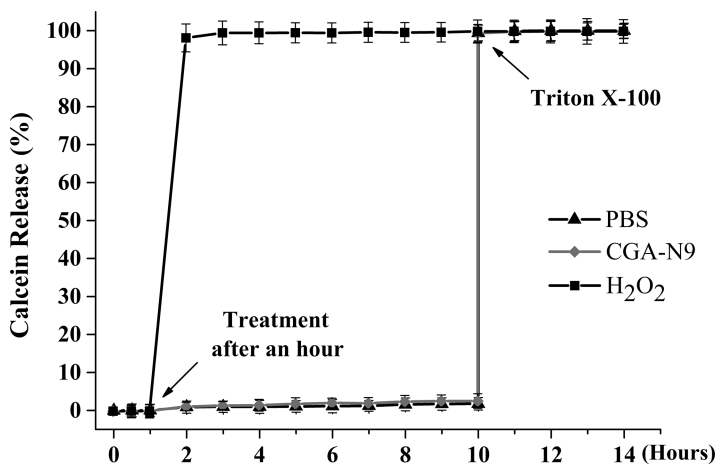

Figure 7. Effect of CGA-N9 on membrane integrity.

Calcein-loaded liposomes were incubated with 3.9 μg/ml CGA-N9 or 0.3% H_2O_2 at 28°C. The fluorescence of calcein released from the liposomes was recorded using a fluorescence spectrophotometer. An increase in fluorescence indicated an increase in membrane permeability. Complete leakage from liposomes was observed upon the addition of the membrane-disrupting agent Triton X-100 (0.1%) at 10 h. Calcein-loaded liposomes that had undergone PBS treatment were used as negative controls. Data represent the mean ± standard deviation of three independent experiments.

Biochemical Journal (2019) **476** 483–497
https://doi.org/10.1042/BCJ20180801

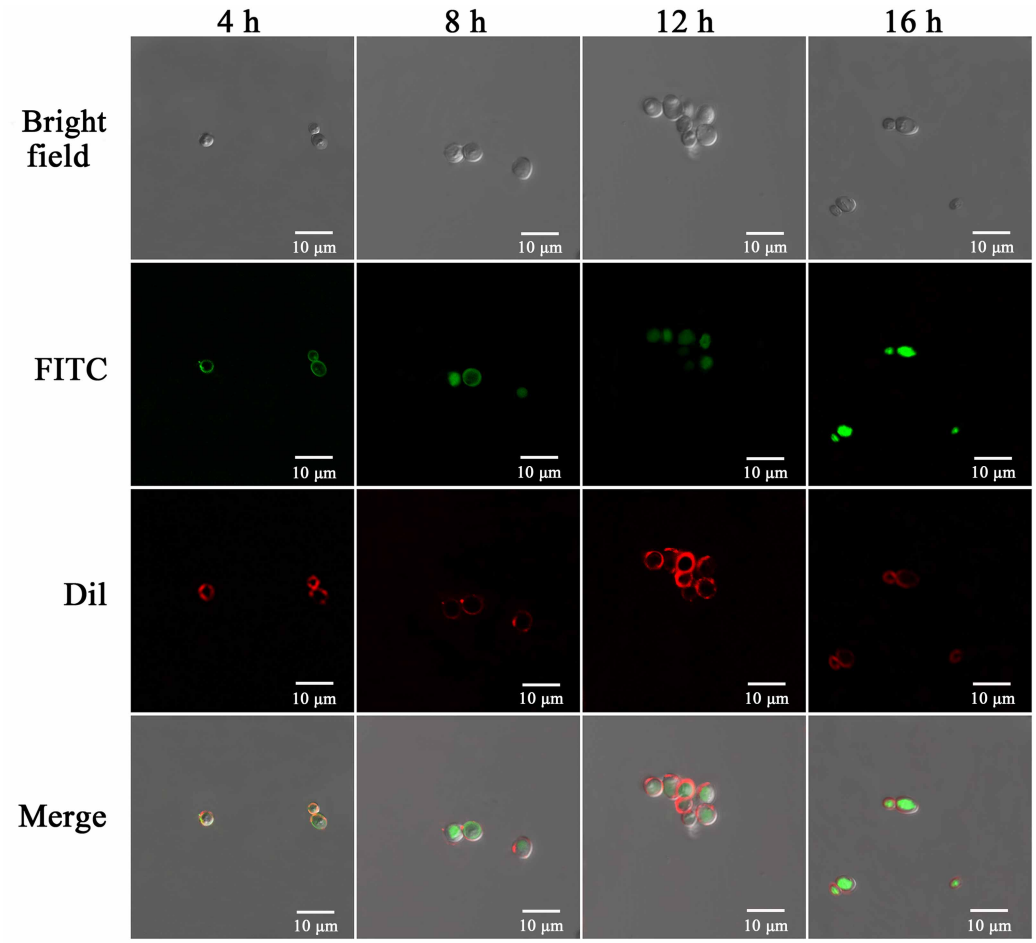

Figure 8. CGA-N9 internalization in *C. tropicalis* cells.

A total of 1×10^6 logarithmic-phase *C. tropicalis* cells were incubated with MIC_{50} of CGA-N9 (2.9 μg/ml) at 28°C for 4, 8, 12 and 16 h. Entry of the FITC-CGA-N9 conjugate into *C. tropicalis* cells was observed using confocal microscopy in cells co-stained with the membrane dye DiI. CGA-N9 entered *C. tropicalis* cells in a time-dependent manner. Initially, the FITC-CGA-N9 conjugate accumulated around the cell membrane. Upon further incubation, FITC-CGA-N9 was translocated into the cytoplasm, as indicated by increased intracellular green fluorescence intensity. Scale bar = 10 μm.

CGA-N9 internalization

Internalization of FITC-labeled peptides into *C. tropicalis* was further examined by laser confocal microscopy, as shown in Figure 8. Confocal microscopy analysis showed that FITC-CGA-N9 was initially localized at the periphery of *C. tropicalis* cells, with further incubation resulting in internalization and intracellular accumulation in a time-dependent manner. CGA-N9 was initially internalized into cells in a nondisruptive manner and subsequently induced cytotoxicity.

Effect of energy on CGA-N9 internalization

An environmental temperature of 4°C blocks all energy-dependent pathways [37], and NaN_3, an inhibitor of cytochrome oxidase in the mitochondrial respiratory chain, can inhibit mitochondrial ATP (adenosine triphosphate) production. In contrast with their behavior at 30°C, the FITC-CGA-N9 conjugate was incompletely internalized into *C. tropicalis* cells after being cultured at 4°C for 12 h. NaN_3 had the same effect as 4°C on the cellular uptake of CGA-N9. As shown by confocal microscopy, although CGA-N9 entered most of the cells, it remained localized at the periphery in some cells, binding only to the membrane (Figure 9). These results

Biochemical Journal (2019) **476** 483–497
https://doi.org/10.1042/BCJ20180801

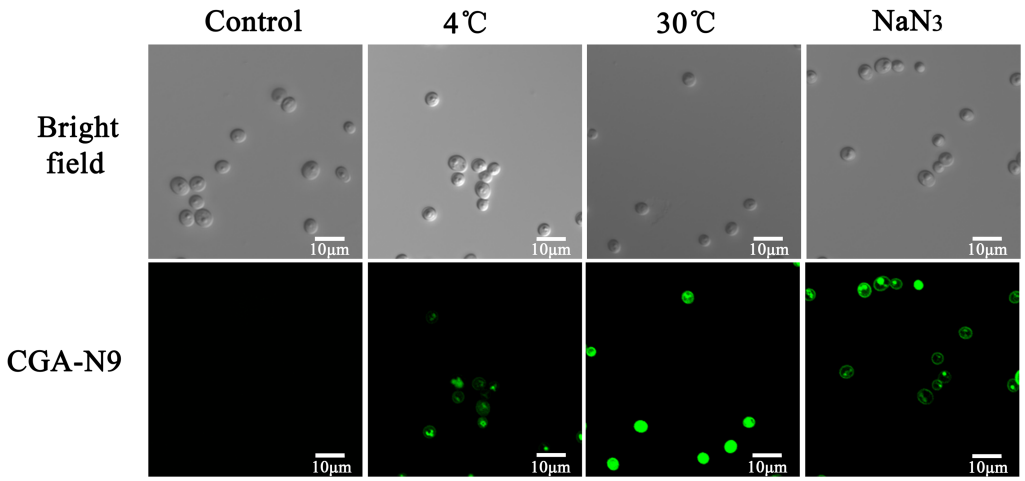

Figure 9. Effect of energy on CGA-N9 internalization.

A total of 1×10^6 logarithmic-phase *C. tropicalis* cells were incubated with the MIC_{50} of CGA-N9 (2.9 μg/ml) for 12 h. Cells in the control group that had not undergone CGA-N9 treatment and in the NaN_3-treated group were cultured at 28°C. Uptake of the FITC-CGA-N9 conjugate was assessed by confocal microscopy. Compared with that at 30°C, cellular uptake of CGA-N9 by *C. tropicalis* cells was partially blocked by 4°C and NaN_3. Scale bar = 10 μm.

confirmed that CGA-N9 internalization mostly involves energy-independent direct cell penetration, with a slight contribution of energy-dependent endocytosis.

Effects of endocytic inhibitors on CGA-N9 internalization

Endocytosis pathways are mediated by many factors, such as cholesterol, Na^+/H^+ ion pumps, clathrin and actin [38,40–42]. Endocytosis inhibitors, such as CPZ, CQ, Mβ-CD, NaN_3, CyD, EIPA and heparin, inhibit these factors to suppress endocytic pathways. CPZ inhibits clathrin-mediated endocytosis, and CQ prevents endocytosis by blocking internal acidification of the endosome. Mβ-CD suppresses pinocytosis through caveolin, NaN_3 disrupts endocytosis by inhibiting mitochondrial ATP production and CyD and EIPA are inhibitors of macropinocytosis. CyD interacts with the cytoskeleton, inhibiting actin polymerization, and EIPA blocks Na^+/H^+ exchange. Heparin is a competitive inhibitor of sulfate proteoglycans on the cell surface that competes with endocytic agents for binding the sulfated-protein receptor, thereby preventing endocytic agents from aggregating on the membrane and reducing endocytosis [38,39,43].

We further explored the relationship between endocytic pathways in *C. tropicalis* cells and CGA-N9. Logarithmic-phase *C. tropicalis* cells were pretreated with CPZ (7.11 μg/ml), CQ (1.72 μg/ml), Mβ-CD (3.75 mg/ml), NaN_3 (0.65 mg/ml), CyD (5.08 μg/ml), EIPA (10 μg/ml) or heparin (100 μg/ml), followed by incubation with 3.9 μg/ml (MIC_{100}) FITC-CGA-N9 conjugate without the removal of the inhibitor. As observed via laser confocal microscopy (Figure 10A) and the recorded FITC fluorescence values (Figure 10B), CQ and Mβ-CD had no effect on cellular uptake of CGA-N9, whereas CPZ, NaN_3, CyD, EIPA and heparin all inhibited uptake. These results suggest that the endocytic pathways involved in CGA-N9 internalization are ATP-dependent macropinocytosis, clathrin-mediated endocytosis and sulfate proteoglycan receptor binding.

Effect of endocytic inhibitors on CGA-N9 cytotoxicity

To further explore the effects of endocytosis inhibitors on CGA-N9-induced cytotoxicity and the primary endocytic pathways involved, logarithmic-phase *C. tropicalis* cells were treated with 1.95, 2.9 and 3.9 μg/ml CGA-N9 in the presence of CPZ (7.11 μg/ml), CQ (1.72 μg/ml), Mβ-CD (3.75 mg/ml), NaN_3 (0.65 mg/ml), CyD (5.08 μg/ml), EIPA (10 μg/ml) or heparin (100 μg/ml), and cell viability was then determined using the MIC assay (Figure 11). Compared with the survival rate of control cells, survival rates were significantly enhanced by treatment with EIPA and heparin, followed by CyD, and then NaN_3 and CPZ. In the CQ- and Mβ-CD-treatment groups, the survival rate of *C. tropicalis* cells was nearly the same as that of the control, suggesting that CQ and Mβ-CD had no effect on CGA-N9 internalization. Moreover, at low CGA-N9

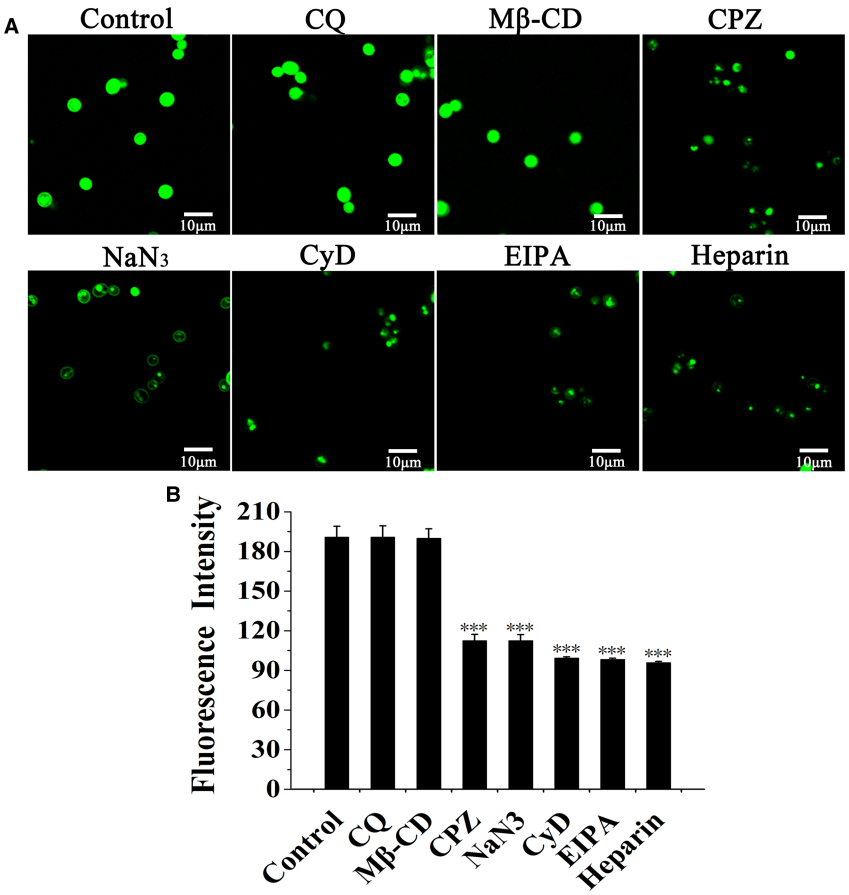

Figure 10. Effects of endocytic inhibitors on CGA-N9 internalization.

A total of 1×10^6 logarithmic-phase *C. tropicalis* cells were incubated with the MIC_{100} of CGA-N9 (3.9 μg/ml) at 28°C for 12 h. Uptake of the FITC-CGA-N9 conjugate by *C. tropicalis* cells in the presence of endocytic inhibitors was assessed (**A**), and the fluorescence intensity of FITC was recorded (**B**) using confocal microscopy, Scale bar = 10 μm. Uptake of the FITC-CGA-N9 conjugate by *C. tropicalis* cells in the absence of endocytic inhibitors was used as the control. Compared with the control, cellular uptake of CGA-N9 by *C. tropicalis* was partially blocked by endocytic inhibitors. Pre-incubation with CyD, an inhibitor of actin polymerization, dramatically blocked the internalization of 3.9 μg/ml CGA-N9. A similar inhibitory effect was observed in cells pretreated with ethylisopropylamiloride (EIPA), a Na^+/H^+ exchange inhibitor, and heparin, a competitive inhibitor of sulfate proteoglycan binding. Additionally, NaN_3 reduced CGA-N9 endocytosis by inhibiting ATP production, and CPZ, a clathrin-dependent endocytosis inhibitor, showed a slight inhibitory effect on CGA-N9 cellular uptake. In contrast, chloroquine (CQ), an endosomal internal acidification inhibitor, and methyl-β-cyclodextrin (Mβ-CD), a caveolae-mediated endocytosis inhibitor, had no effect on cell penetration by CGA-N9. Data represent the mean ± standard deviation of three independent experiments. ***$P < 0.001$ (Student's *t*-test).

concentrations, the primary endocytic pathway was mediated by heparin, followed by EIPA and then CyD. At killing concentrations of CGA-N9, CPZ and NaN_3 also exhibited some effect. The results indicate that CGA-N9 entered the cells partly via the endocytosis pathway in an ATP-dependent manner; in contrast, endocytic inhibitors, with the exception of CQ and Mβ-CD, partially ameliorated the cytotoxicity of CGA-N9 in *C. tropicalis*.

Discussion

CGA-N9 displays antimicrobial activity, particularly *C. tropicalis*, with high safety in HRBCs and mouse brain microvascular endothelial cells. Here, the cytotoxicity of this peptide against *C. tropicalis* is investigated based on the routes by which CGA-N9 crosses cell membranes.

Biochemical Journal (2019) **476** 483–497
https://doi.org/10.1042/BCJ20180801

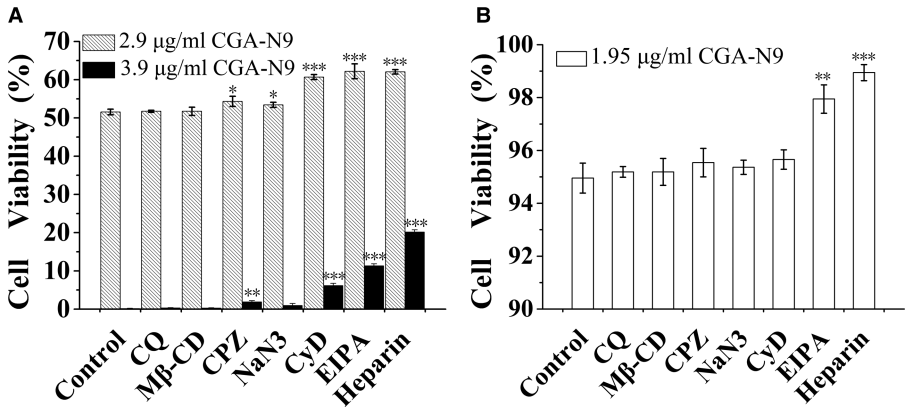

Figure 11. Effects of endocytic inhibitors on the antifungal activity of CGA-N9.

A total of 1×10^6 logarithmic-phase *C. tropicalis* cells were incubated with CGA-N9 at 28°C for 16 h at concentrations of 3.9 μg/ml (MIC_{100}) and 2.9 μg/ml (MIC_{50}) (**A**) and 1.95 μg/ml (MIC_5) (**B**). The antifungal activity of CGA-N9 against *C. tropicalis* cells in the presence of endocytic inhibitors was assessed using the MIC assay. The antifungal activity of CGA-N9 against *C. tropicalis* cells in the absent of endocytic inhibitors was used as a control. Compared with the control, pre-incubation with heparin, a competitive binding inhibitor of sulfate proteoglycans, dramatically blocked CGA-N9 activity. Inhibitory effects were also detected in cells pretreated with ethylisopropylamiloride (EIPA), a Na^+/H^+ exchange inhibitor, and CyD, an inhibitor of actin polymerization. Additionally, CPZ, a clathrin-dependent endocytosis inhibitor, and NaN_3, an ATP production inhibitor, partly reduced CGA-N9 endocytosis. In contrast, CQ, an endosomal internal acidification inhibitor, and methyl-β-cyclodextrin (Mβ-CD), a caveolae-mediated endocytosis inhibitor, had no effect on the penetration of CGA-N9. It is interesting that EIPA and heparin showed primary inhibitory activity at low CGA-N9 concentrations. Data represent the mean ± standard deviation of three independent experiments. $^*P < 0.05$, $^{**}P < 0.01$, $^{***}P < 0.001$ (Student's *t*-test).

The membrane activity of AMPs can be roughly divided into two categories: membrane destruction and non-membrane destruction. Most AMPs kill bacteria by destroying the cell membrane, though a few kill microbes via non-membrane destruction [44,45]. In this study, CGA-N9, a hydrophobic peptide with no typical structural characteristics, killed *C. tropicalis* in a time-dependent manner without destroying the integrity of the cell membrane, including an absence of pore formation.

Numerous studies have investigated the membrane processes associated with cell-penetrating peptides (CPPs) [46,47], the entry pathways of which are classified into two groups: energy-independent direct penetration and energy-dependent endocytosis [48–50].

The direct penetration process has unique features; for example, it is not only energy-independent but also occurs at low temperatures and in the presence of endocytic inhibitors [50]. Direct penetration across the cell membrane primarily occurs in cases involving high concentrations of highly basic and arginine-rich peptides [40,51,52]. In this study, cellular internalization of CGA-N9 by *C. tropicalis* cells was assessed using an FITC-CGA-N9 conjugate at 4°C and in the presence of NaN_3 at a concentration of 2.9 μg of CGA-N9/ml (MIC_{50}). Our results showed incomplete internalization of the peptide in *C. tropicalis* cells under these conditions.

Endocytosis is a natural and energy-dependent process that occurs in all cells and may occur via several different pathways: macropinocytosis, clathrin- or caveolin-mediated endocytosis or clathrin-/caveolin-independent endocytosis [47,51,53–55]. The endocytic inhibitors CyD, EIPA, heparin and CPZ inhibit endocytosis pathways by different mechanisms. In our investigation, CyD, EIPA, heparin and CPZ also influenced CGA-N9 internalization, indicating that CGA-N9 internalization is associated with the macropinocytosis pathway, sulfate proteoglycans on the cell surface and the clathrin-dependent endocytosis pathway. At concentrations below the MIC_{50}, the macropinocytosis pathway is the primary endocytic pathway for CGA-N9, a conclusion also supported by its antimicrobial activity. In addition, CPZ and NaN_3reduced the antimicrobial activity of CGA-N9, though their effect was reduced compared with that of EIPA, heparin or CyD.

Overall, a single CPP can exploit different routes to enter cells and these routes may occasionally operate concomitantly, depending on the differing physicochemical properties, sizes and concentrations of diverse CPPs [56–58]. Based on the results of our CGA-N9 internalization experiments, except for a few peptides that

require ATP for internalization, CGA-N9 molecules pass through the cell membrane via direct penetration. That is, energy-independent direct penetration is the primary internalization pathway, accompanied by energy-dependent macropinocytosis, sulfate proteoglycan-mediated endocytosis and weak clathrin-mediated endocytosis.

Studies have revealed that arginine residues contribute more to cellular uptake than do lysines [44,59,60]. The 9-amino-acid sequence of CGA-N9 contains two arginine residues, and these residues facilitate peptide binding to the membrane through electrostatic interactions.

In conclusion, CGA-N9 appears to first bind to the cell membrane through electrostatic forces, after which it passes through the membrane via direct penetration, accompanied by macropinocytosis, sulfate proteoglycan-mediated endocytosis and weak clathrin-mediated endocytosis with ATP consumption.

Abbreviations

AMPs, antimicrobial peptides; ATCC, American Type Culture Collection; ATP, adenosine triphosphate; bEnd.3, mouse brain microvascular endothelial cell line; CCK8, cell counting kit-8; Cfu, colony forming unit; CGA, chromogranin A; CGA-N9, the sequence from the 47th to the 55th amino acid of the N-terminus of chromogranin A; CPP, cell-penetrating peptide; CPZ, chlorpromazine; CQ, chloroquine; CyD, cytochalasin D; EIPA, 5-(*N*-ethyl-*N*-isopropyl)-amiloride; FITC, fluorescein isothiocyanate; HRBCs, human red blood cells; LB, Luria-Bertani; MFC, minimum fungicidal concentration; MIC, minimum inhibitory concentration; MTT, 3-(4,5-dimethylthiazol-2-yl)-2,5-diphenyltetrazolium; Mβ-CD, methyl-β-cyclodextrin; NaN_3, sodium azide; PBS, phosphate-buffered saline; PI, propidium iodide; SD, Sabouraud dextrose; SPSS, statistical product and service solutions; TEM, transmission electron microscopy.

Author Contribution

Ruifang Li drafted the manuscript and participated in the design and coordination of the experiments. Chen Chen carried out the experiments and drafted the manuscript. Sha Zhu provided guidance for the experiments. Xueqin Wang and Yanhui Yang participated in the final editing of the manuscript. Weini Shi, Sijia Chen, Congcong Wang, Lixing Yan and Jiaofan Shi participated in the experiments. All authors have read and approved the final manuscript.

Funding

The National Natural Science Foundation of China (31071922 and 31572264), the Innovative Research Team (in Science and Technology) at the University of Henan Province (19IRTSTHN008), the Fundamental Research Funds for Henan Provincial Colleges and Universities at the Henan University of Technology (2015RCJH03), the Henan Provincial Science and Technology Research Project (162102310404) and the National Engineering Laboratory for Wheat and Corn Further Processing at the Henan University of Technology (NL2016010) all provided financial support for the authors.

Competing Interests

The Authors declare that there are no competing interests associated with the manuscript.

References

1 Yapar, N. (2014) Epidemiology and risk factors for invasive candidiasis. *Ther. Clin. Risk Manag.* **10**, 95–105 https://doi.org/10.2147/TCRM.S40160
2 Lovero, G., De Giglio, O., Montagna, O., Diella, G., Divenuto, F., Lopuzzo, M. et al. (2016) Epidemiology of candidemia in neonatal intensive care units: a persistent public health problem. *Ann. Ig.* **28**, 282–287 https://doi.org/10.7416/ai.2016.2107
3 Yang, Y., Guo, F., Kang, Y., Zang, B., Cui, W., Qin, B. et al. (2017) Epidemiology, clinical characteristics, and risk factors for mortality of early- and late-onset invasive candidiasis in intensive care units in China. *Medicine* **96**, e7830 https://doi.org/10.1097/MD.0000000000007830
4 Kothavade, R.J., Kura, M.M., Valand, A.G. and Panthaki, M.H. (2010) *Candida tropicalis*: its prevalence, pathogenicity and increasing resistance to fluconazole. *J. Med. Microbiol.* **59**, 873–880 https://doi.org/10.1099/jmm.0.013227-0
5 Chai, L.Y., Denning, D.W. and Warn, P. (2010) *Candida tropicalis* in human disease. *Crit. Rev. Microbiol.* **36**, 282–298 https://doi.org/10.3109/1040841X.2010.489506
6 Zuza-Alves, D.L., Silva-Rocha, W.P. and Chaves, G.M. (2017) An update on *Candida tropicalis* based on basic and clinical approaches. *Front. Microbiol.* **8**, 1927 https://doi.org/10.3389/fmicb.2017.01927
7 da Silva, A.R., de Andrade Neto, J.B., da Silva, C.R., Campos Rde, S., Costa Silva, R.A., Freitas, D.D. et al. (2016) Berberine antifungal activity in fluconazole-resistant pathogenic yeasts: action mechanism evaluated by flow cytometry and biofilm growth inhibition incandidaspp. *Antimicrob. Agents Chemother.* **60**, 3551–3557 https://doi.org/10.1128/AAC.01846-15
8 Yeaman, M.R. and Yount, N.Y. (2003) Mechanisms of antimicrobial peptide action and resistance. *Pharmacol. Rev.* **55**, 27–55 https://doi.org/10.1124/pr.55.1.2

Biochemical Journal (2019) **476** 483–497
https://doi.org/10.1042/BCJ20180801

9 Burrows, L.L., Stark, M., Chan, C., Glukhov, E., Sinnadurai, S. and Deber, C.M. (2006) Activity of novel non-amphipathic cationic antimicrobial peptides against *Candida* species. *J. Antimicrob. Chemother.* **57**, 899–907 https://doi.org/10.1093/jac/dkl056

10 Dong, W., Mao, X., Guan, Y., Kang, Y. and Shang, D. (2017) Antimicrobial and anti-inflammatory activities of three chensinin-1 peptides containing mutation of glycine and histidine residues. *Sci. Rep.* **7**, 40228 https://doi.org/10.1038/srep40228

11 Desbois, A.P., Tschörner, D. and Coote, P.J. (2011) Survey of small antifungal peptides with chemotherapeutic potential. *Curr. Pharm. Biotechnol.* **12**, 1263–1291 https://doi.org/10.2174/138920111796117265

12 De Lucca, A.J. and Walsh, T.J. (2000) Antifungal peptides: origin, activity, and therapeutic potential. *Rev. Iberoam. Micol.* **17**, 116–120 PMID:15762805

13 Ng, T.B. (2004) Antifungal proteins and peptides of leguminous and non-leguminous origins. *Peptides* **25**, 1215–1222 https://doi.org/10.1016/j.peptides.2004.03.012

14 Wiesner, J. and Vilcinskas, A. (2010) Antimicrobial peptides: the ancient arm of the human immune system. *Virulence* **1**, 440–464 https://doi.org/10.4161/viru.1.5.12983

15 Meyer, V. and Jung, S. (2018) Antifungal peptides of the AFP family revisited: are these cannibal toxins? *Microorganisms* **6**, 50 https://doi.org/10.3390/microorganisms6020050

16 Simon, J.P. and Aunis, D. (1989) Biochemistry of the chromogranin A protein family. *Biochem. J.* **262**, 1–13 https://doi.org/10.1042/bj2620001

17 Lugardon, K., Raffner, R., Goumon, Y., Corti, A., Delmas, A., Bulet, P. et al. (2000) Antibacterial and antifungal activities of Vasostatin-1, the N-terminal fragment of chromogranin A. *J. Biol. Chem.* **275**, 10745–10753 https://doi.org/10.1074/jbc.275.15.10745

18 Aslam, R., Atindehou, M., Lavaux, T., HaïKel, Y., Schneider, F. and Metz-Boutigue, M.H. (2012) Chromogranin A-derived peptides are involved in innate immunity. *Curr. Med. Chem.* **19**, 4115–4123 https://doi.org/10.2174/092986712802430063

19 Naito, A., Matsumori, N. and Ramamoorthy, A. (2018) Dynamic membrane interactions of antibacterial and antifungal biomolecules, and amyloid peptides, revealed by solid-state NMR spectroscopy. *Biochim. Biophys. Acta* **1862**, 307–323 https://doi.org/10.1016/j.bbagen.2017.06.004

20 Travkova, O.G., Moehwald, H. and Brezesinski, G. (2017) The interaction of antimicrobial peptides with membranes. *Adv. Colloid Interface Sci.* **247**, 521–532 https://doi.org/10.1016/j.cis.2017.06.001

21 Garibotto, F.M., Garro, A.D., Masman, M.F., Rodríguez, A.M., Luiten, P.G., Raimondi, M. et al. (2010) New small-size peptides possessing antifungal activity. *Bioorg. Med. Chem.* **18**, 158–167 https://doi.org/10.1016/j.bmc.2009.11.009

22 Kondejewski, L.H., Jelokhani-Niaraki, M., Farmer, S.W., Lix, B., Kay, C.M., Sykes, B.D. et al. (1999) Dissociation of antimicrobial and hemolytic activities in cyclic peptide diastereomers by systematic alterations in amphipathicity. *J. Biol. Chem.* **274**, 13181–13192 https://doi.org/10.1074/jbc.274.19.13181

23 Cudic, M. and Otvos, L. (2002) Intracellular targets of antibacterial peptides. *Curr. Drug Targets* **3**, 101–106 https://doi.org/10.2174/1389450024605445

24 Zore, G.B., Thakre, A.D., Jadhav, S. and Karuppayil, M. (2011) Terpenoids inhibit *Candida albicans* growth by affecting membrane integrity and arrest of cell cycle. *Phytomedicine* **18**, 1181–1190 https://doi.org/10.1016/j.phymed.2011.03.008

25 Wang, K., Yan, J., Dang, W., Xie, J., Yan, B., Yan, W. et al. (2014) Dual antifungal properties of cationic antimicrobial peptides polybia-MPI: membrane integrity disruption and inhibition of biofilm formation. *Peptides* **56**, 22–29 https://doi.org/10.1016/j.peptides.2014.03.005

26 Muñoz, A., Gandía, M., Harries, E., Carmoa, L., Read, N.D. and Marcos, J.F. (2013) Understanding the mechanism of action of cell-penetrating antifungal peptides using the rationally designed hexapeptide PAF26 as a model. *Fungal Biol. Rev.* **26**, 146–155 https://doi.org/10.1016/j.fbr.2012.10.003

27 Hu, K., Jiang, Y., Xie, Y., Liu, H., Liu, R., Zhao, Z. et al. (2015) Small-anion selective transmembrane 'holes' induced by an antimicrobial peptide too short to span membranes. *J. Phys. Chem. B* **119**, 8553–8560 https://doi.org/10.1021/acs.jpcb.5b03133

28 Li, R.-F., Yan, X.-H., Lu, Y.-B., Lu, Y.-L., Zhang, H.-R., Chen, S.-H. et al. (2015) Anti-candidal activity of a novel peptide derived from human chromogranin A and its mechanism of action against *Candida krusei*. *Exp. Ther. Med.* **10**, 1768–1776 https://doi.org/10.3892/etm.2015.2731

29 Sun, Y., Dong, W., Sun, L., Ma, L. and Shang, D. (2015) Insights into the membrane interaction mechanism and antibacterial properties of chensinin-1b. *Biomaterials* **37**, 299–311 https://doi.org/10.1016/j.biomaterials.2014.10.041

30 Li, R.-F., Lu, Y.-L., Lu, Y.-B., Zhang, H.-R., Huang, L., Yin, Y.-L. et al. (2015) Antiproliferative effect and characterization of a novel antifungal peptide derived from human Chromogranin A. *Exp. Ther. Med.* **10**, 2289–2294 https://doi.org/10.3892/etm.2015.2838

31 Mishra, B., Wang, X., Lushnikova, T., Zhang, Y., Golla, R.M., Narayana, J.L. et al. (2018) Antibacterial, antifungal, anticancer activities and structural bioinformatics analysis of six naturally occurring temporins. *Peptides* **106**, 9–20 https://doi.org/10.1016/j.peptides.2018.05.011

32 Li, S., Chen, J.-X., Xiang, Q.-X., Zhang, L.-Q., Zhou, C.-H., Xie, J.-Q. et al. (2014) The synthesis and activities of novel mononuclear or dinuclear cyclen complexes bearing azole pendants as antibacterial and antifungal agents. *Eur. J. Med. Chem.* **84**, 677–686 https://doi.org/10.1016/j.ejmech.2014.07.075

33 Yang, Q., Yin, Y., Yu, G., Jin, Y., Ye, X., Shrestha, A. et al. (2015) A novel protein with anti-metastasis activity on 4T1 carcinoma from medicinal fungus *Cordyceps militaris*. *Int. J. Biol. Macromol.* **80**, 385–391 https://doi.org/10.1016/j.ijbiomac.2015.06.050

34 Li, R., Zhang, R., Yang, Y., Wang, X., Yi, Y., Fan, P. et al. (2018) CGA-N12, a peptide derived from chromogranin A, promotes apoptosis of *Candida tropicalis* by attenuating mitochondrial functions. *Biochem. J.* **475**, 1385–1396 https://doi.org/10.1042/BCJ20170894

35 Lattif, A.A., Mukherjee, P.K., Chandra, J., Roth, M.R., Welti, R. and Rouabhia, M. (2011) Lipidomics of *Candida albicans* biofilms reveals phase-dependent production of phospholipid molecular classes and role for lipid rafts in biofilm formation. *Microbiology* **157**, 3232–3242 https://doi.org/10.1099/mic.0.051086-0

36 Ruissen, A.L., Groenink, J., Helmerhorst, E.J., Walgreen-Weterings, E., Van't Hof, W., Veerman, E.C. et al. (2001) Effects of histatin 5 and derived peptides on *Candida albicans*. *Biochem. J.* **356**, 361–368 https://doi.org/10.1042/bj3560361

37 Pushpanathan, M., Rajendhran, J., Jayashree, S., Sundarakrishnan, B., Jayachandran, S. and Gunasekaran, P. (2012) Direct cell penetration of the antifungal peptide, mmgp1, in *Candida albicans*. *J. Pept. Sci.* **18**, 657–660 https://doi.org/10.1002/psc.2445

38 Wang, C., Dong, S., Lin, Z., Ying, Z., Huang, L., Gong, X. et al. (2017) Cell surface binding, uptaking and anticancer activity of l-k6, a lysine/leucine-rich peptide, on human breast cancer mcf-7 cells. *Sci. Rep.* **7**, 8293 https://doi.org/10.1038/s41598-017-08963-2

39 Saha, K., Kim, S.T., Yan, B., Miranda, O.R., Alfonso, F.S., Shlosman, D. et al. (2013) Surface functionality of nanoparticles determines cellular uptake mechanisms in mammalian cells. *Small* **9**, 300–305 https://doi.org/10.1002/smll.201201129

40 Duchardt, F., Fotinmleczek, M., Schwarz, H., Fischer, R. and Brock, R. (2007) A comprehensive model for the cellular uptake of cationic cell-penetrating peptides. *Traffic* **8**, 848–866 https://doi.org/10.1111/j.1600-0854.2007.00572.x
41 Poole, B. and Ohkuma, S. (1981) Effect of weak bases on the intralysosomal pH in mouse peritoneal macrophages. *J. Cell Biol.* **90**, 665–669 https://doi.org/10.1083/jcb.90.3.665
42 Aghamohammadzadeh, S., Smaczynska-de Rooij, I.I. and Ayscough, K.R. (2014) An abp1-dependent route of endocytosis functions when the classical endocytic pathway in yeast is inhibited. *PLoS ONE* **9**, e103311 https://doi.org/10.1371/journal.pone.0103311
43 Tian, T., Zhu, Y.L., Zhou, Y.Y., Liang, G.F., Wang, Y.Y. and Hu, F.H. (2014) Exosome uptake through clathrin-mediated endocytosis and macropinocytosis and mediating mir-21 delivery. *J. Biol. Chem.* **289**, 22258–22267 https://doi.org/10.1074/jbc.M114.588046
44 Wimley, W.C. (2010) Describing the mechanism of antimicrobial peptide action with the interfacial activity model. *ACS Chem. Biol.* **5**, 905–917 https://doi.org/10.1021/cb1001558
45 Mahlapuu, M., Håkansson, J., Ringstad, L. and Björn, C. (2016) Antimicrobial peptides: an emerging category of therapeutic agents. *Front. Cell. Infect. Microbiol.* **6**, 194 https://doi.org/10.3389/fcimb.2016.00194
46 Oh, E., Delehanty, J.B., Sapsford, K.E., Susumu, K., Goswami, R., Blanco-Canosa, J.B. et al. (2011) Cellular uptake and fate of PEGylated gold nanoparticles is dependent on both cell-penetration peptides and particle size. *ACS Nano.* **8**, 6434–6448 https://doi.org/10.1021/nn201624c
47 Koren, E. and Torchilin, V.P. (2012) Cell-penetrating peptides: breaking through to the other side. *Trends Mol. Med.* **7**, 385–393 https://doi.org/10.1016/j.molmed.2012.04.012
48 Richard, J.P., Melikov, K., Vives, E., Ramos, C., Verbeure, B., Gait, M.J. et al. (2003) Cell-penetrating peptides. *J. Biol. Chem.* **3**, 585–590 https://doi.org/10.1074/jbc.M209548200
49 Farkhani, S.M., Valizadeh, A., Karami, H., Mohammadi, S., Sohrabi, N. and Badrzadeh, F. (2014) Cell penetrating peptides: efficient vectors for delivery of nanoparticles, nanocarriers, therapeutic and diagnostic molecules. *Peptides* **57**, 78–94 https://doi.org/10.1016/j.peptides.2014.04.015
50 Guidotti, G., Brambilla, L. and Ross, D. (2017) Cell-penetrating peptides: from basic research to clinics. *Trends Pharmacol. Sci.* **38**, 406–424 https://doi.org/10.1016/j.tips.2017.01.003
51 Fretz, M.M., Penning, N.A., Al-Tael, S., Futakl, S., Takeuchi, T., Nakase, I. et al. (2007) Temperature-, concentration- and cholesterol-dependent translocation of L- and D-octa-arginine across the plasma and nuclear membrane of CD34^{+} leukaemia cells. *Biochem. J.* **403**, 335–342 https://doi.org/10.1042/BJ20061808
52 Kosuge, M., Takeuchi, T., Nakase, I., Jones, A.T. and Futaki, S. (2008) Cellular internalization and distribution of arginine-rich peptides as a function of extracellular peptide concentration, serum, and plasma membrane associated proteoglycans. *Bioconjug. Chem.* **19**, 656–664 https://doi.org/10.1021/bc700289w
53 Lundberg, M., Wikström, S. and Johansson, M. (2003) Cell surface adherence and endocytosis of protein transduction domains. *Mol. Ther.* **8**, 143–150 https://doi.org/10.1016/S1525-0016(03)00135-7
54 Hirose, H., Takeuchi, T., Osakada, H., Pujals, S., Katayama, S., Nakase, I. et al. (2012) Transient focal membrane deformation induced by arginine-rich peptides leads to their direct penetration into cells. *Mol. Ther.* **20**, 984–993 https://doi.org/10.1038/mt.2011.313
55 Pang, H.-B., Braun, G.B., Friman, T., Aza-Blanc, P., Ruidiaz, M.E., Sugahara, K.N. et al. (2014) An endocytosis pathway initiated through neuropilin-1 and regulated by nutrient availability. *Nat. Commun.* **5**, 4904 https://doi.org/10.1038/ncomms5904
56 Nakase, I., Takeuchi, T., Tanaka, G. and Futaki, S. (2008) Methodological and cellular aspects that govern the internalization mechanisms of arginine-rich cell-penetrating peptides. *Adv. Drug Deliv. Rev.* **60**, 598–607 https://doi.org/10.1016/j.addr.2007.10.006
57 Takeshima, K., Chikushi, A., Lee, K.K., Yonehara, S. and Matsuzaki, K. (2003) Translocation of the analogues of antimicrobial peptides Maiganin and Buforin across human cell membranes. *J. Biol. Chem.* **278**, 1310–1315 https://doi.org/10.1074/jbc.M208762200
58 Komin, A., Russell, L.M., Hristova, K.A. and Searson, P.C. (2017) Peptide-based strategies for enhanced cell uptake, transcellular transport, and circulation: mechanisms and challenges. *Adv. Drug Deliv. Rev.* **110-111**, 52–64 https://doi.org/10.1016/j.addr.2016.06.002
59 Rothbard, J.B., Kreider, E., VanDeusen, C.L., Wright, L., Wylie, B.L. and Wender, P.A. (2002) Arginine-rich molecular transporters for drug delivery: role of backbone spacing in cellular uptake. *J. Med. Chem.* **45**, 3612–3618 https://doi.org/10.1021/jm0105676
60 Tünnemann, G., Ter-Avetisyan, G., Martin, R.M., Stöckl, M., Herrmann, A. and Cardoso, M.C. (2010) Live-cell analysis of cell penetration ability and toxicity of oligo-arginines. *J. Pept. Sci.* **14**, 469–476 https://doi.org/10.1002/psc.968